

Reporting Kinetics and Dynamics of Phase Transitions of 8OCB Liquid Crystal using Logger Pro

Grace Petrarca

Undergraduate student, Emmanuel College, Boston, MA, 02115 USA

Dipti Sharma (PhD)

Supervisor, Emmanuel College, Boston, MA 02115 USA

Abstract

This research examines the kinetics and dynamics of phase transitions of 4-oxy-4'-cyano-biphenyls (8OCB) Liquid Crystal (LC). In this study, detailed results are focused on the effect of ramp rates of phase transitions of 8OCB. The sample of 8OCB was heated from -40 °C to 100 °C and then cooled back from 100 °C to -40 °C with three different 5 °C/min, 10 °C/min, and 20 °C/min ramp rates using Differential Scanning Calorimetry (DSC). The 8OCB shows four phases and three-phase transitions. These phases are crystalline (K), Smectic A (SmA), Nematic (N), and Isotropic (I). The phase transitions of 8OCB are K-SmA, SmA-N, N-I. Each phase transition of 8OCB is detectable and appears in DSC scans. These peak temperatures of each phase transition shift with the increasing ramp rates. While heating, all phase transitions move towards higher temperatures. During cooling, all the phase transitions move towards lower temperatures when the ramp rate is increased. Each of the phase transitions shows activated kinetics with the presence of activation energy which is energy required by 8OCB molecules to be activated in that phase while they are heated or cooled. The crystallization state shows double peaks, and it appears in both heating and cooling, so we decided to call "Krytallization" (K) heat crystallization whereas Crystallization (C) is cooling crystallization. These kinetic results can be explained in terms of the Arrhenius Model. The detailed values of heat capacity, activation energy, and entropy of each transition peak are reported in this paper to further show how distinct changes in 8OCB occur.

Keywords: Differential Scanning Calorimetry, crystalline, smectic A, nematic, isotropic specific heat capacity, activation energy, wing jump, kinetics, dynamics, liquid crystals, ramp rates.

Date of Submission: 01-04-2025

Date of acceptance: 11-04-2025

I. Introduction

There are traditionally three states of matter: solid, liquid, and gases. Molecules transition between the states of matter based on an increase or decrease in energy in a system to allow or restrict an atom's freedom of movement.[1] However, there are intermediate states of matter. Liquid crystal molecules (LCs) possess a unique property that allows them to display distinct phase changes between the transition of solid (crystalline) and liquid (isotropic). LCs, in general, exist on the spectrum of crystalline, Smectic C, Smectic A, Nematic, and isotropic. There are three main types of LCs: thermotropic, lyotropic, and metallotropic.[2] Lyotropic are LCs most affected by temperature and concentration, usually in a water solvent. Metallotropics are LCs that combine both inorganic and organic materials whose behavior highly depends on the concentration of inorganic material. Finally, thermotropic LCs specifically are the type of liquid crystals that are highly affected by changes in temperature and the most relevant in technological applications like liquid crystal displays (LCDs). [3-4] The properties of LCs and how they apply to the application LCDs can be analyzed using Differential Scanning Calorimetry (DSC). DSC was used to study the thermodynamic behavior of liquid crystals to determine their phase change and behavior. DSC detects the phase change of liquid crystals by measuring heat flow versus temperature within the material.[5]

LCD is a type of display that uses liquid crystals, characteristic of being polymorphic. An important phenomenon that permits LCDs to work is a 90° orientation of two layers of liquid crystal that allows polarized light to be twisted and pass through the two polarizers to the pixel and create an image. [6] This technique has revolutionary technology compared to its predecessor, the cathode ray tube monitors. The n(O)CB family has become a significant discovery in LCD research, with the liquid crystal phase being discovered by Austrian botanist Friedrich Reinitzer in 1888 to great controversy.[7] After further exploration, the LC was discovered to

have its own set of subphases that have been integral in LCD, the most important of which has been the nematic phase. Nematic LCs are a phase in the transition of an LC from crystalline to isotropic. Specifically relating to technology, LCDs utilize the nematic phase of LCs when applying an electric field to advantage the needed optical properties. [8-9]

8OCB is an organic, biphenyl structure with octyloxy and cyano groups at 4,4'-positions (4-oxy-4'-cyano-biphenyls). The molecular formula is $C_{21}H_{25}ON$. 8OCB differs from the nCB family by adding oxygen in the CB tail.[10] Both 8OCB and 8CB have similar phase transitions, however, the addition of oxygen increases the stability of the dipole moment induced through a hydrogen-bond network via the CN groups, therefore stabilizing the phases of the LC at higher temperatures relative to 8CB. [11-13] The 8OCB's characteristics can be quantitatively represented through the program LoggerPro to further understand its potential. LoggerPro by Vernier is a data analysis software designed to compile data from different data collection apparatuses. LoggerPro is an experimental software in many academic institutions to evaluate and interpret real-world data in undergraduate research settings.[14]

The interest at hand is further exploring the thermodynamic properties of 8OCB and how its structure influences different phenomena seen with LoggerPro's graphical analysis capabilities. Having a better understanding of 8OCB can aid in how the advantages of 8OCB can be manipulated in developing technologies. One of the issues plaguing LCD is LC integrity over time. As LCs within LCDs are constantly being manipulated by an inducible electrical current and the temperature of the surrounding environment, the LCs often become impure and unable to handle the influx of energy over time. This can cause pixel misalignment and an overall lack of screen quality. 8OCB has been known to be a partially stable LC and reliable in handling variable energy fluctuation in LCD. [15-16] Through the investigation of the activation energy, heat capacity, and enthalpy, different thermodynamic phenomena will be explored to better understand effects of continuous heating and cooling of 8OCB. This research will explore 8OCB as a strong candidate to be further integrated into LCD manufacturing, especially regarding technology needed in environments without constant temperature control that requires affordable and reliable technology.

II. Materials and Methods

8OCB is a thermotropic liquid crystal of the nOCB family. **Figure 1** shows oxygen characteristically linking the Octyloxy and Biphenyl groups, giving rise to specific behavior only observed by the nOCB family. **Figure 2** outlines the four significant phase changes 8OCB encounters during heating and cooling; however, this paper will explore the idiosyncratic effects of these phases when repeatedly heated and cooled.

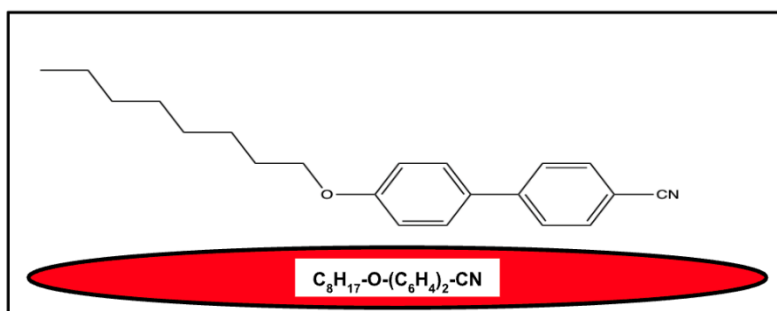


Figure 1. 2D rendering of 8OCB Liquid Crystal Molecule.

The molecular weight of 8OCB is 307.43 g/mol. In this study, 5.0 mg of 8OCB was taken in an aluminum cup and then sealed with its lid as part of the apparatus that is used to study the thermal behavior of 8OCB. The instrument used for this study is called Differential Scanning Calorimetry (DSC). The sealed cup and lid with 8OCB sample was then taken into the DSC, model 214 instrument from the NETZSCH company at WPI, chemistry and biochemistry department, Worcester, MA. This sample of 8OCB was heated from $-40\text{ }^\circ\text{C}$ to $100\text{ }^\circ\text{C}$ and then cooled back from $100\text{ }^\circ\text{C}$ to $-40\text{ }^\circ\text{C}$ with three different $5\text{ }^\circ\text{C}/\text{min}$, $10\text{ }^\circ\text{C}/\text{min}$, and $20\text{ }^\circ\text{C}/\text{min}$ heating and cooling ramp rates. The data collected from the DSC produced data to show how heat flows in the sample with time and temperature. This data was taken to Logger Pro for further detailed analysis of 8OCB thermal behavior. The thermal behavior of 8OCB was analyzed isothermally (when the temperature of the sample is changed, and corresponding heat flow is measured) and then computationally manipulated to explore heat capacity (C_p) and the relationship between activation energy (E_a) and the subsequent rate of the reaction to examine the effect of heating and reheating on LC 8OCB. Further information on the Hf and non-isothermal effects of continuously heating and cooling 8OCB can be found in other studies [17].

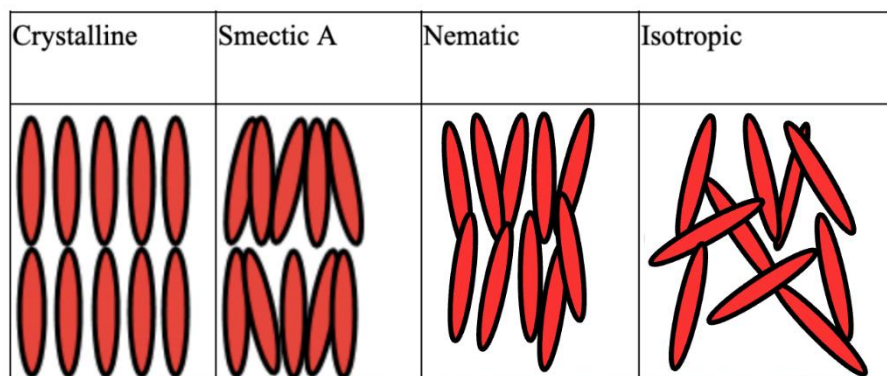


Figure 2. The molecular arrangement of 8OCB LC in four phases as seen in the heating and cooling in Crystalline (C), Smectic A (SmA), Nematic (N), and Isotropic (I).

III. Theory

A. Specific Heat Capacity and Enthalpy of Phase Transitions

In thermodynamics, heat (Q) relates to the mass of the sample (m), its specific heat capacity (C_p), and the change in temperature (ΔT), as shown in equation 1. As the DSC measures heat flow instead of just heat, the heat flow (dQ/dt) can be shown as a function of heating rate (dT/dt) in equation 2.

$$Q = m * C_p * \Delta T \quad (1)$$

$$\frac{dQ}{dT} = m * C_p * \frac{dT}{dt} \quad (2)$$

Rearranging the second equation can provide the specific heat capacity of a substance,

$$C_p = \frac{1}{m} * \frac{dT}{dt} * \frac{dQdt}{dT} \quad (3)$$

Change in Enthalpy (ΔH) represents the total internal energy change of the LC during heating and cooling. This relationship is derived from the integration of the C_p vs T graph,

$$\Delta H = \int C_p * dt \quad (4)$$

Equations 1-4 have the following units: dQ/dt or Heat Flow is in Watts or J/s. After establishing the HF was in W/g, specific heat capacity units could be concluded as of J/g°C. Mass was measured in grams, time in seconds, and temperature in °C.

B. Kinetics of Phase Transitions

To further study the effects of reheating and cooling 8OCB, the Arrhenius equation that relates the rate of a reaction to its activation energy is given:

$$k = A e^{-\frac{E_a}{RT}} \quad (5)$$

Where k is the rate of the experiment, A is a pre-exponential factor, E_a is the activation energy, R is the universal gas constant, and T is the temperature. Equation 4 can be related to this research:

$$\beta = \beta_0 e^{-\frac{E_a}{RT}} \quad (6)$$

Where β is the ramp rate, β_0 is a constant, E_a is the activation energy, R is the universal gas constant, and T is temperature. The natural log of equation 5 will produce a linear reference for further data exploration.

The natural log of equation 5 relates the equation to the linear equation of a line:

$$\ln(\beta) = \ln(\beta_0) - \frac{E_a}{RT} \quad (7)$$

Further rearrangement yields:

$$\ln(\beta) = \left(-\frac{E_a}{RT}\right) * 1/T + \ln(\beta_0) \quad (8)$$

Resembling the equation of a line:

$$y = -mx + b \quad (9)$$

As y is the vertical-axis value, m is the slope of the line, x is the value of the horizontal axis, and b is, therefore, the intercept of the y-axis. Due to the similarities of equations 7 and 8:

$$m = \frac{E_a}{RT}, \quad b = \ln(\beta_0) \quad (10)$$

Therefore, the activation energy is represented as equation 10:

$$E_a = m * R \quad (11)$$

IV. Results

A. DSC Results analyzed using Logger Pro

The following data from the DSC instrument was plotted and analyzed using the program. Logger Pro demonstrates intricate changes shown by 8OCB when repeatedly heated and cooled at increasing rates.

Figure 3 represents the heating of 8OCB in the DSC instrument for all three ramp rates of 5, 10, and 20°C/min. The “K” represents 8OCB molecules being in a state of crystalline before the heating, whereas the “I” represents the liquid molecules being in a state of isotropic, completely melted after heating. **Figure 4** represents the cooling of these liquid crystal molecules at the same three ramp rates and could be seen to include additional peaks in the crystalline phase transition of the graph. It is also worth knowing that in **Figure 3**, there is an additional heating crystalline Peak for 20°C/min ramp rate. Both of the graphs have heat capacity compared to the temperature of the phase transition. The heat capacity was calculated from the heat flow as seen in equation 3 in the thermodynamic relationship of mass, heat capacity, heat flow, and change in temperature. The Cp was calculated by multiplying the normalized heat flow by the reciprocal of the specific heat rate for each trial.

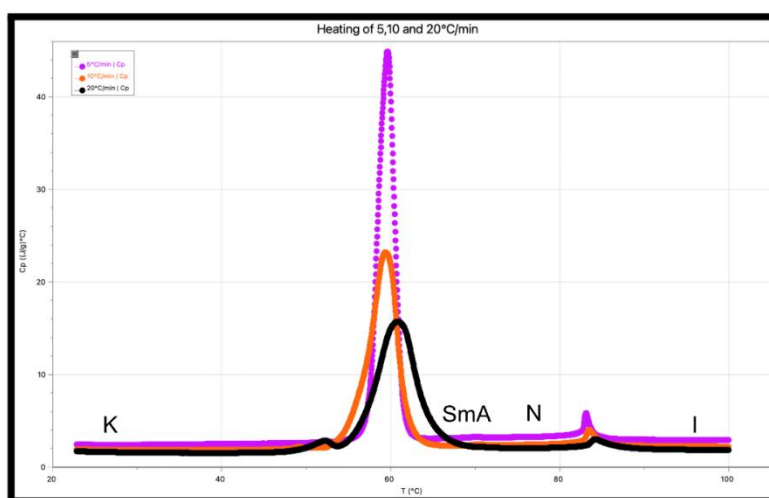


Figure 3. Specific Heat Capacity (Cp) Vs Temperature (T) plot of all phase transitions of 8OCB in heating with three 5°C/min, 10°C/min, and 20°C/min ramp rates.

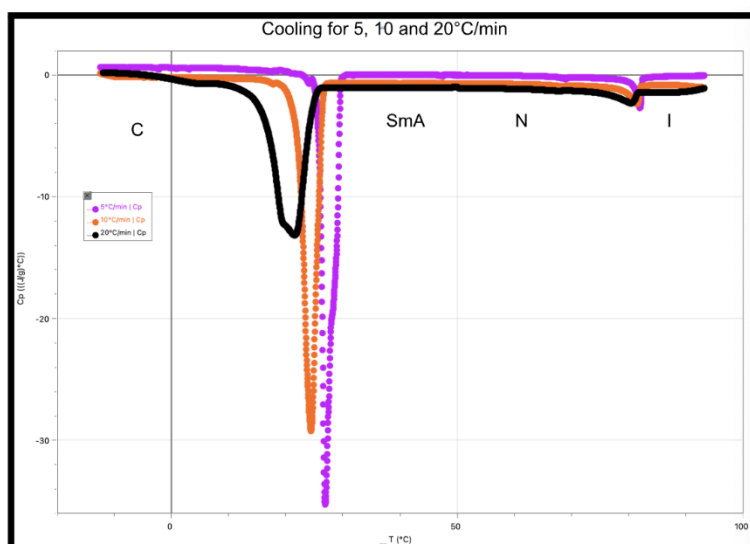


Figure 4. Specific Heat Capacity (C_p) Vs Temperature (T) plot of all phase transitions of 8OCB in cooling with three 5°C/min, 10°C/min, and 20°C/min ramp rates.

The peak temperatures for these phase transitions are recorded in **Table 1** found below and catalog the changing kinetics and dynamics that will be explored in further data exploration in understanding how transitions move when energy is repeatedly taken in and out of a system. The table below records the peak temperature values that were shown by 8OCB during heating in the DSC. The uppercase T represents the peak temperature: TK_0 and TK_1 are the peak temperature of the heating crystallization peak, TA is the melting transition peak for smectic A, and TN is the peak temperature of the nematic heating transition. These peaks mark phase transition points in the heating of 8OCB and will showcase when the phase transition occurred during the three different consecutive headings.

Table 1. Peak Temperatures of crystallization peak for heating for three ramp rates of 5, 10, and 20°C/min.

Heating Rate (°C/min)	Peak Temperatures (°C)			
	TK_0	TK_1	TA	TN
5		44.91	69.79	83.12
10	49.19	51.39	70.26	83.49
20	52.39	60.85	70.59	84.19

Table 2 below records the peak temperature values that 8OCB showed during cooling in the DSC. The uppercase T means the peak temperature: TC_0 , TC_1 , and TC_2 are the peak temperatures of the crystallization peak, TA is the cooling transition peak for smectic A, and TN is the peak temperature of the nematic cooling transition. These peaks mark phase transition points in the heating of 8OCB and will showcase when the phase transition occurred during the three different and consecutive cooling.

Table 2. Peak Temperatures for heating of 8OCB for ramp rates of 5, 10, and 20°C/min.

Cooling Rate (°C/min)	Peak (°C)				
	TN	TA	TC_0	TC_1	TC_2
5	81.94	68.99	27.91	26.91	24.09
10	81.41	68.52		24.40	17.83
20	80.41	67.80		21.60	19.59

The relationship between increasing and decreasing peak temperatures will be further explored in relation to the capacity and enthalpy of the system. **Table 1** and **Table 2** showcase movement in the peak transition phases,

indicating the molecules are being affected by repeatedly being heated. The inclusion and disappearance of specific peak transitions during increasing ramp rates also indicate significant physical changes in the molecules themselves. Specifically, in the heating of 8OCB, there is the gain of the second heating crystallization peak, and in the cooling, there is the loss of the crystallization 0 peak.

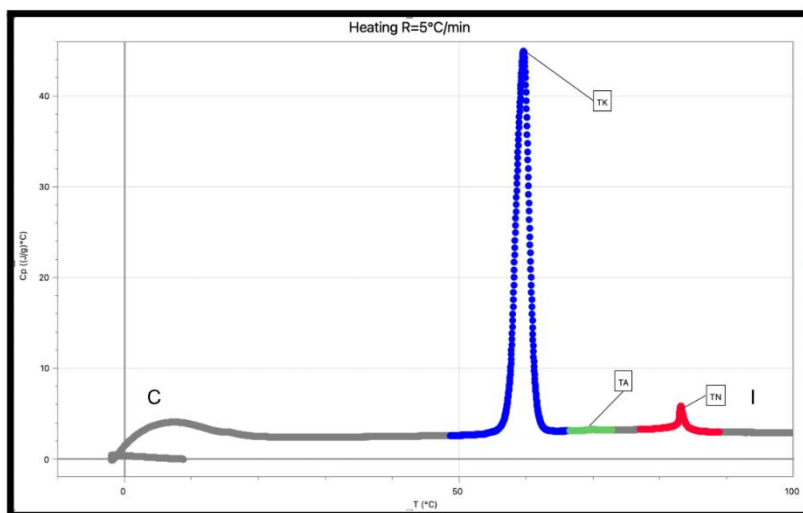


Figure 5. Heating scan of 8OCB at 5°C/min ramp rate. TK, TA, TN represent the crystalline, smectic A, and nematic peaks respectively.

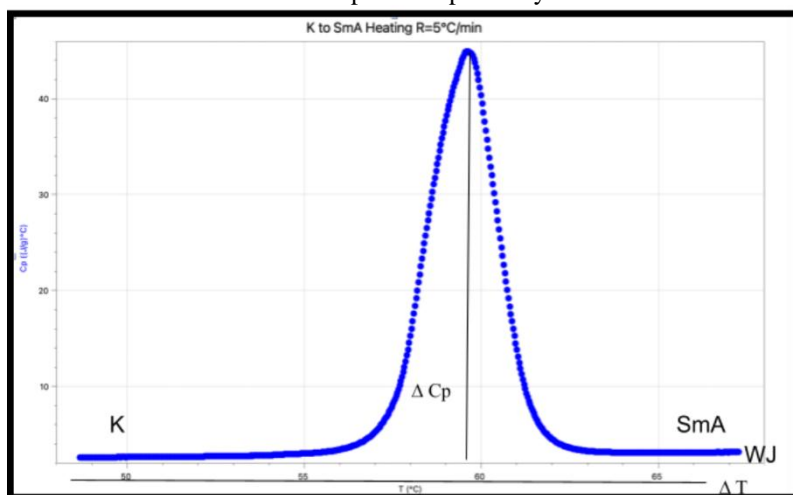


Figure 6. Zoomed-in graph of K-SmA heating transition of 5°C/min.

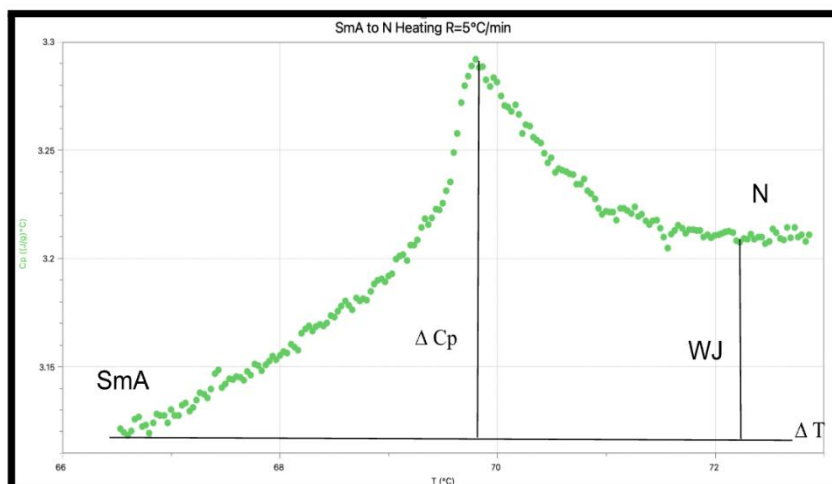


Figure 7. Zoomed-in graph of SmA - N heating transition of 5°C/min.

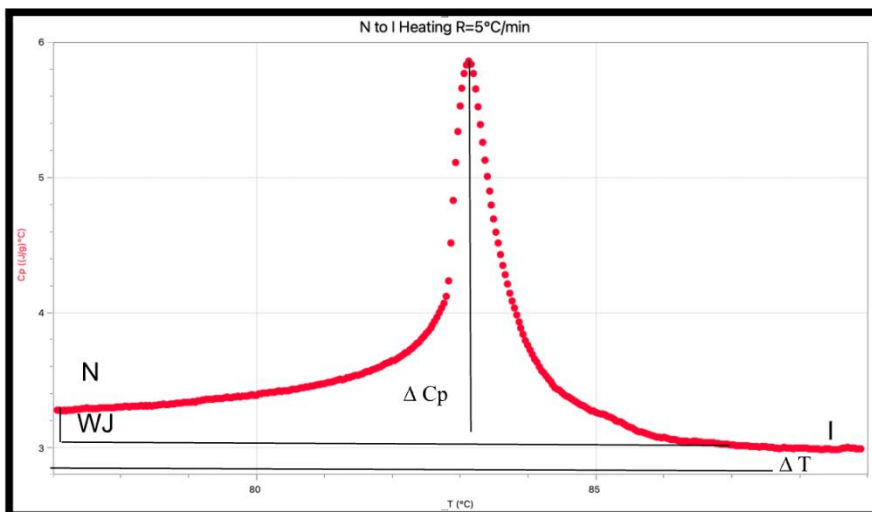


Figure 8. Zoomed-in graph of N-I heating transition of 5°C/min.

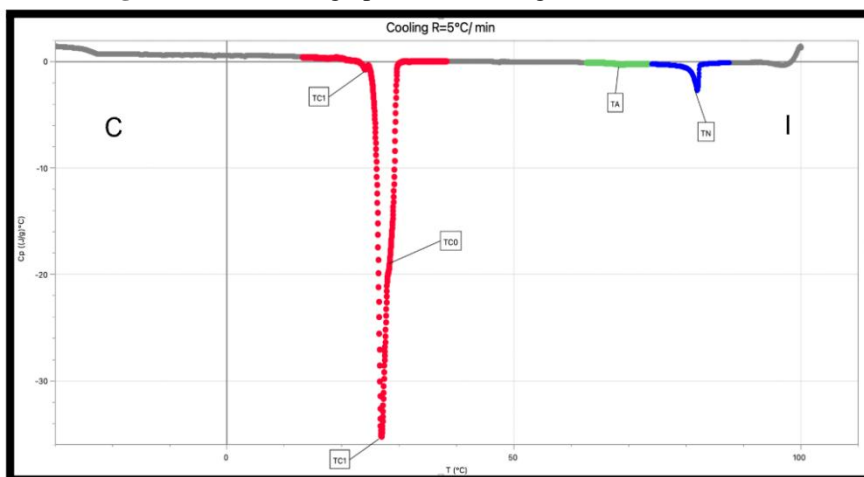


Figure 9. Cooling scan of 8OCB at 5°C/min ramp rate. TC, TA, TN represent the crystalline, smectic A, and nematic peaks respectively.

Figures 5 and Figure 9 represent the entire heating and cooling at a ramp rate of 5°/min for 8OCB subsequent figures represent the zoomed-in phase transitions for ramp rate 5. The relationship between the duration of temperature for the peak, the height of the peak, and the difference between the starting and ending plateau of the transitions are showcased in Table 4, further revealing the effects of exothermic and endothermic differences in increasing ramp rates. As can be seen in Figure 5, there is a stark contrast in the height of the transition peaks, and Figures 7 and 11 demonstrate the differences in the starting and ending Cp for the molecules because of the energy in the system.

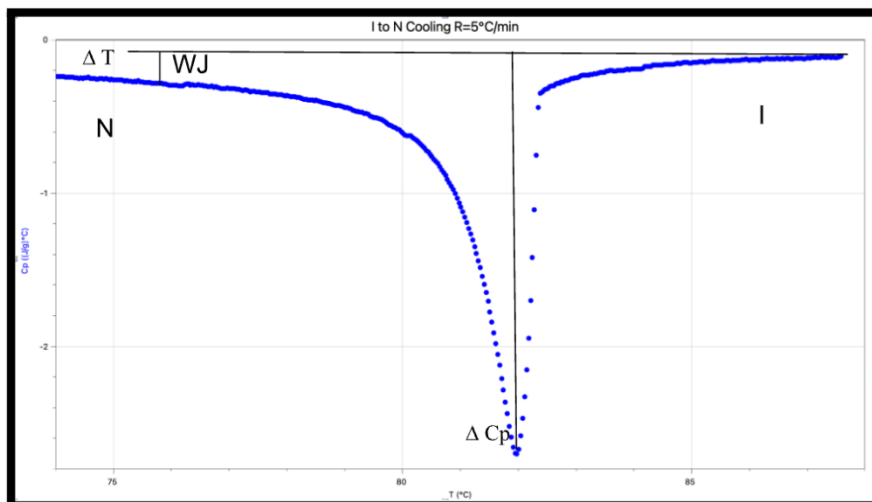


Figure 10. Zoomed-in graph of I -N cooling transition of 5°C/min.

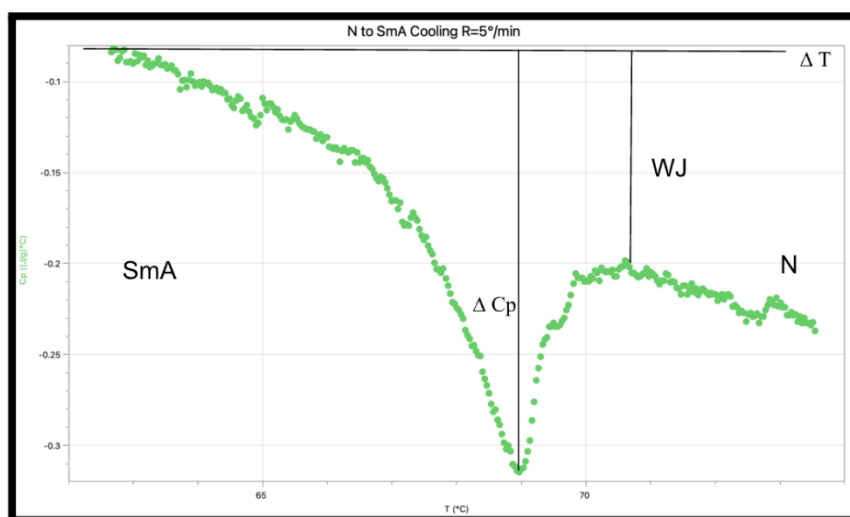


Figure 11. Zoomed-in graph of N -SmA cooling transition of 5°C/min.

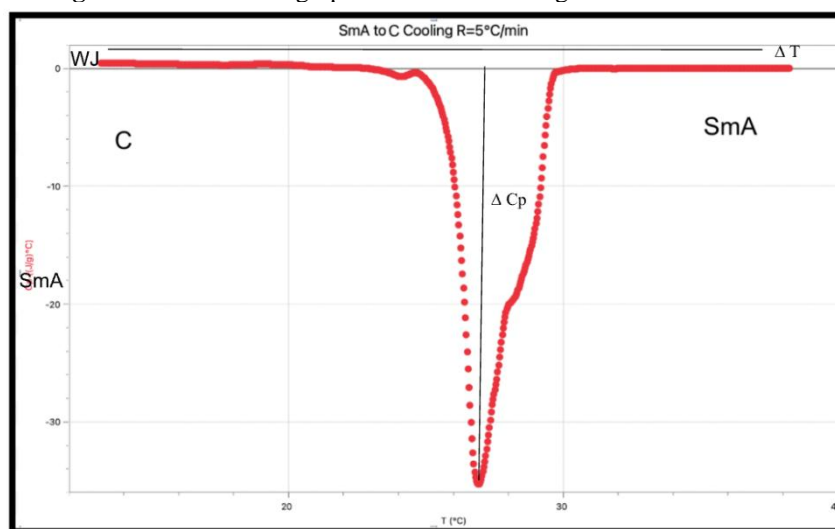


Figure 12. Zoomed in the graph of SmA - C cooling transition of 5°C/min.

B. Effect of Ramp Rates on each phase transition of 8OCB

To understand the effect of the ramp rates on all the phase transitions, summary graphs are plotted that compare and further analyze data from all the phase transitions are plotted below. **Figure 13** and **Figure 14** represent the original data collected from the DSC, where the molecule's heat flow was measured compared to the temperature during the ramp rate.

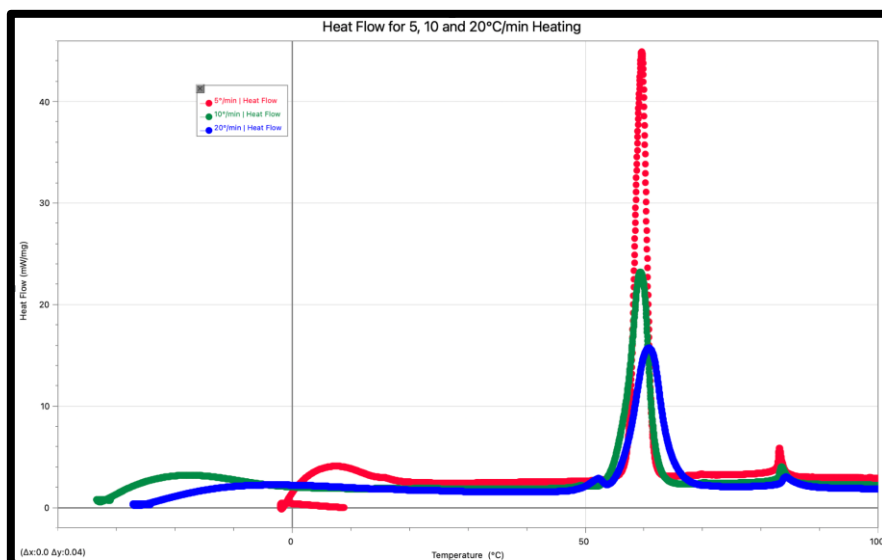


Figure 13. Heat flow vs Temperature plot for heating of 8OCB for 3 different ramp rates: 5°C/min (red), 10°C/min (green), and 20°C/min.

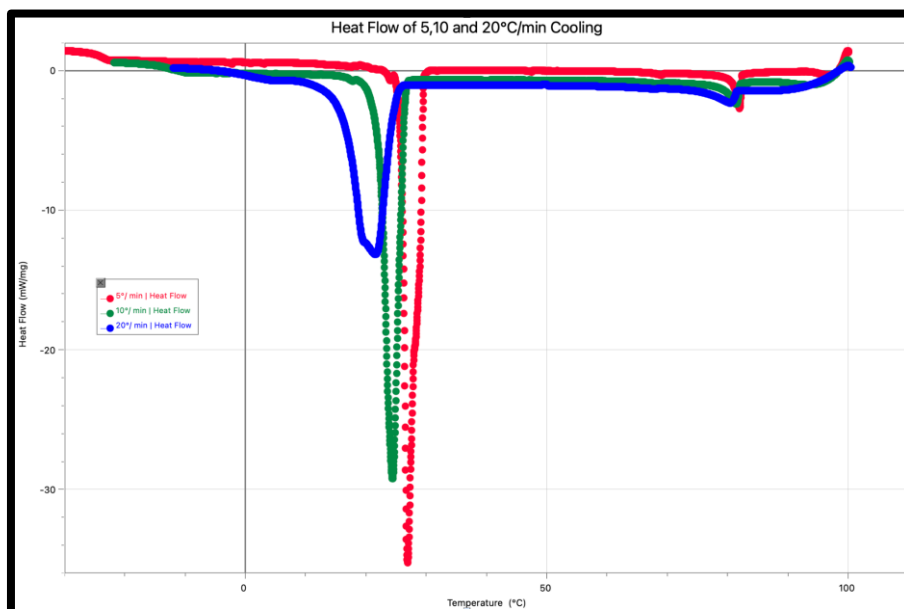


Figure 14. Heat flow vs Temperature plot for cooling of 8OCB for 3 different ramp rates: 5°C/min (red), 10°C/min (green), and 20°C/min.

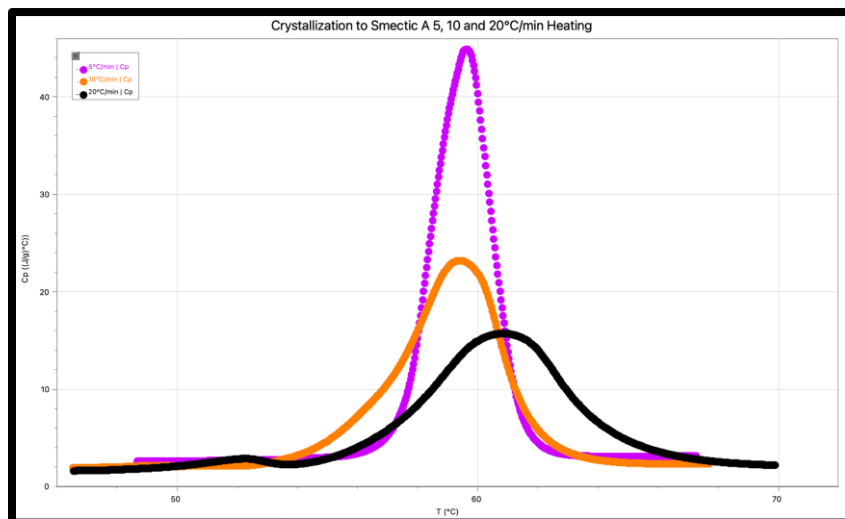


Figure 15. Zoomed-in graph for heating phase transitions of crystalline to smectic A for all three ramp rates 5 (pink), 10 (orange), and 20 (black) $^\circ\text{C}/\text{min}$.

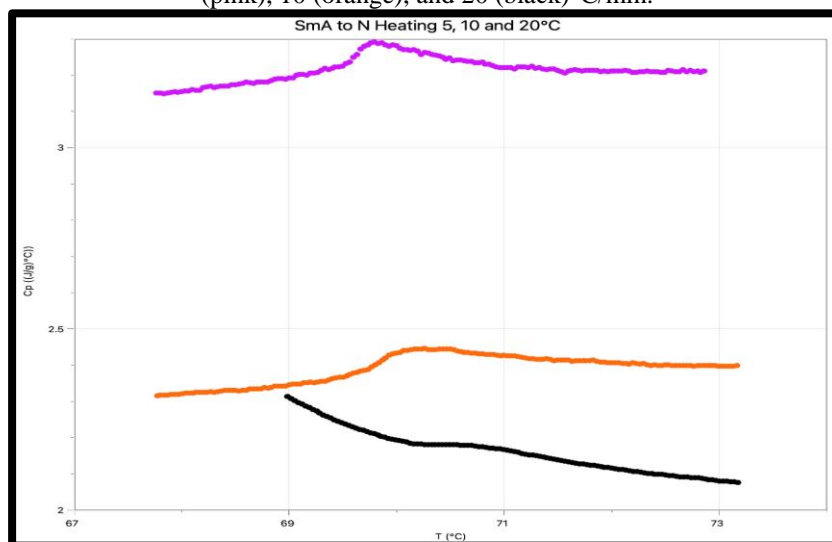


Figure 16. Zoomed in graph for heating phase transitions of smectic A to nematic for all three ramp rates 5 (pink), 10 (orange), and 20 (black) $^\circ\text{C}/\text{min}$.

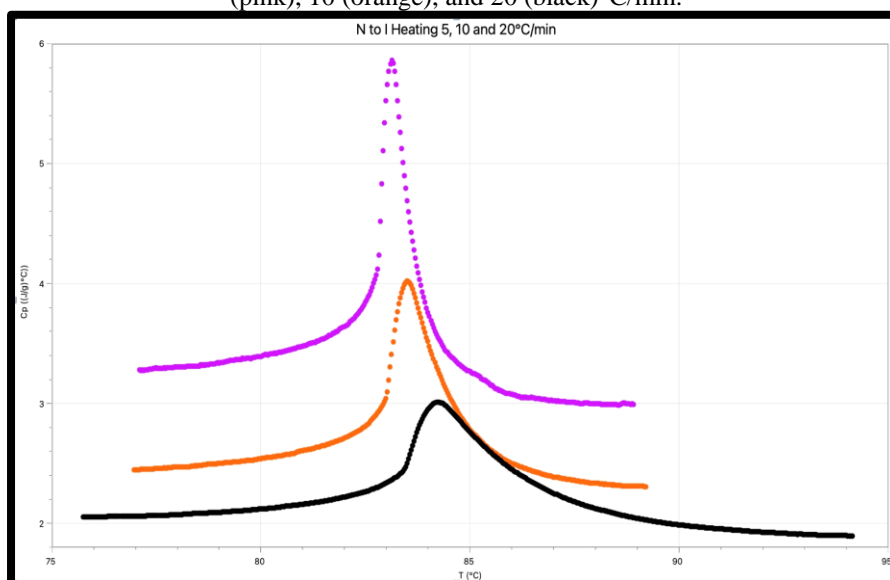


Figure 17. Zoomed in graph for heating phase transitions of nematic to isotropic for all three ramp rates 5 (pink), 10 (orange), and 20 (black) $^\circ\text{C}/\text{min}$.

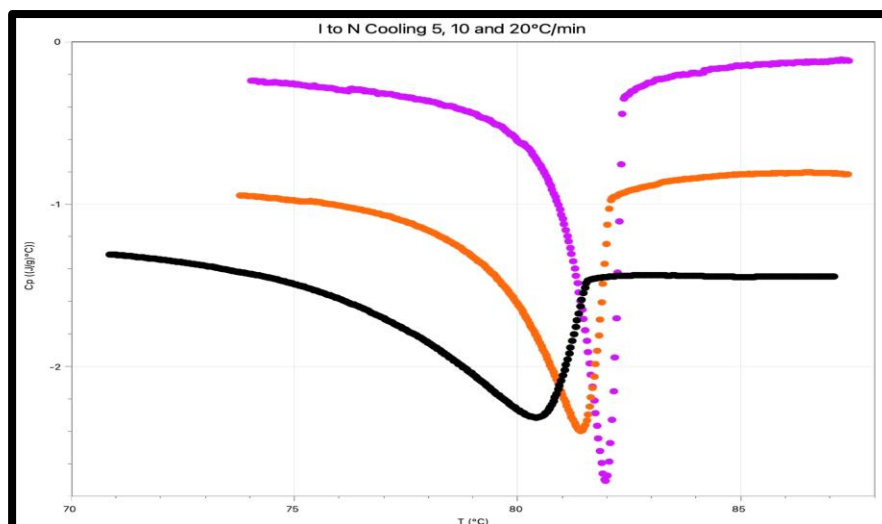


Figure 18. Zoomed in graph for cooling phase transitions of isotropic to nematic for all three ramp rates 5 (pink), 10 (orange), and 20 (black)°C/min.

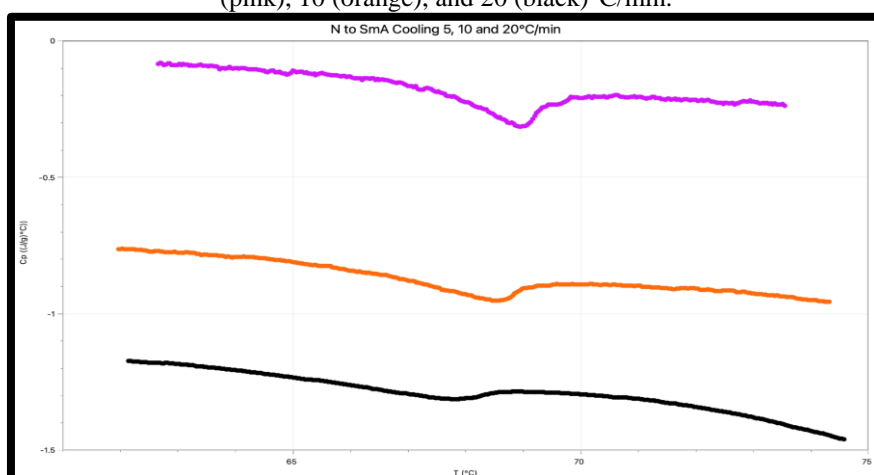


Figure 19. Zoomed in graph for cooling phase transitions of nematic to smectic A for all three ramp rates 5 (pink), 10 (orange), and 20 (black)°C/min.

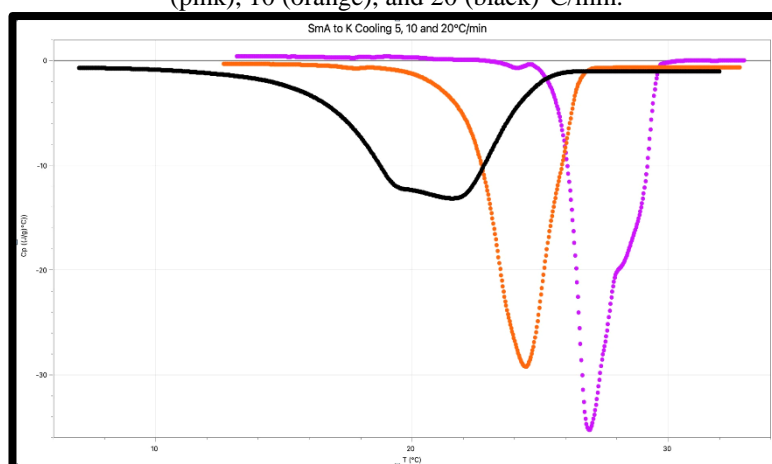


Figure 20. Zoomed in graph for cooling phase transitions of smectic A to crystalline for all three ramp rates 5 (pink), 10 (orange), and 20 (black)°C/min.

As seen in Figures 13-14, the molecules undergo distinctive phase changes marked by transitions representing energy released or absorbed by the system. This overall relates to the alignments of the molecules as a transition from solid, crystalline states to melted, isotropic states. In Figure 13, the heating of liquid molecules presents endothermic heat flow peaks that represent the absorption of energy when transitioning to an increasingly liquid phase. Figure 14 catalogs exothermic heat flow peaks relating to energy being released in the transition of

the phases. **Figures 15-20** are the zoomed-in transitions of 8OCB at all three ramp rates separated by each phase transition during heating and cooling.

C. Presence of Activated Kinetics in 8OCB

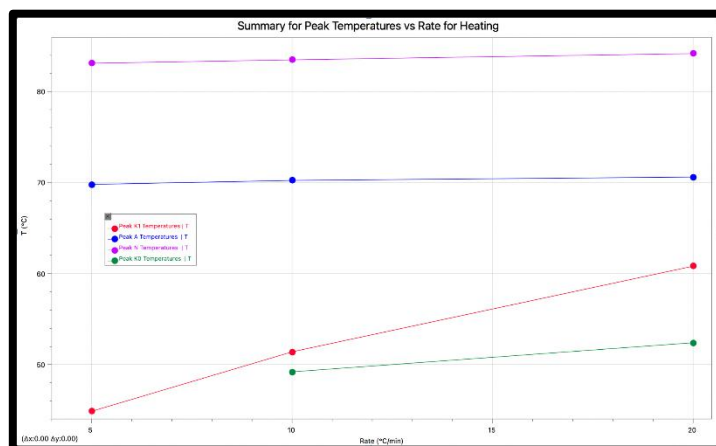


Figure 21. Peak position vs ramp rate plot for heating to show how the peak position of each transition is moving with various ramp rates.

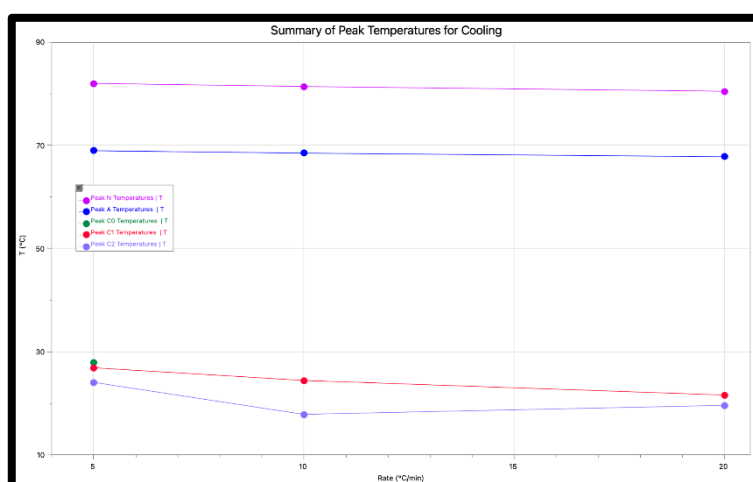


Figure 22. Peak position vs ramp rate plot for cooling to show how the peak position of each transition is moving with various ramp rates.

Figure 21 and **Figure 22** importantly reveal the physical movement of the peak transition temperatures during the increasing ramp rates. This is an extremely important explanation for the kinetics of 8OCB due to the fact that the physical phase transitions do not remain the same when repeatedly heated and cooled. When 8OCB is reheated during ramp rates 10 and 20, phase transitions notably occur at slightly higher temperatures, as seen in **Figure 21**. Whereas when 8OCB is repeatedly cooled in ramp rates of 10 and 20, the phase transition occurs at increasingly lower temperatures as seen in **Figure 22**.

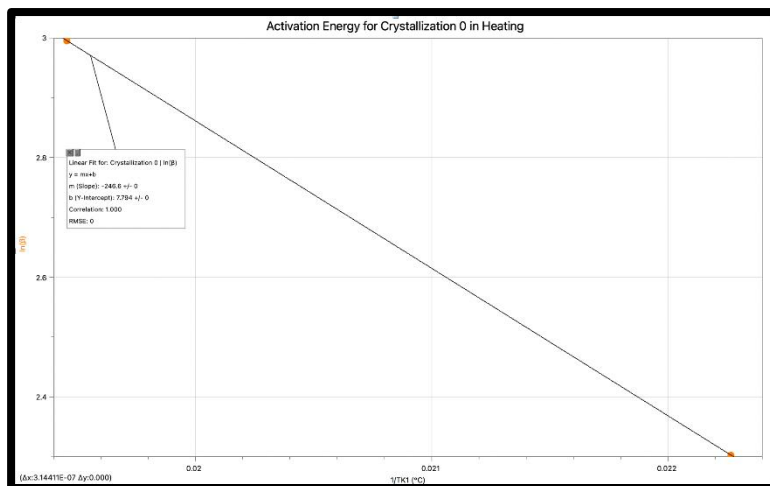


Figure 23. Arrhenius Plot for Crystallization peak in heating showing presence of activation energy in K0

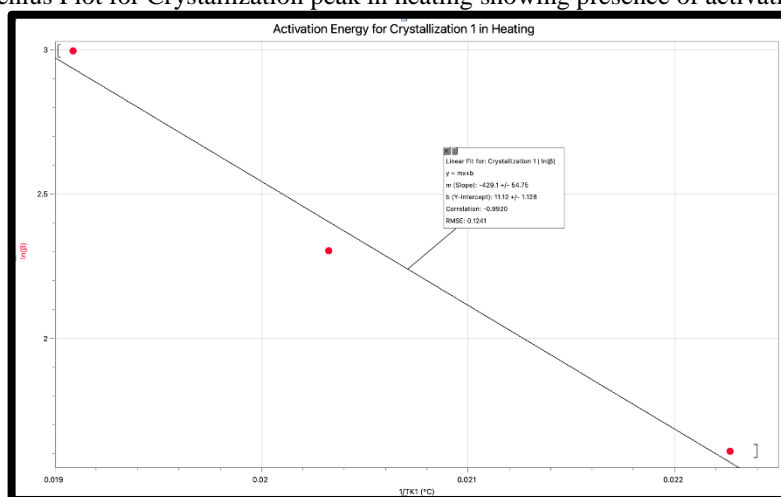


Figure 24. Arrhenius Plot for Crystallization peaks in heating showing presence of activation energy in K1.

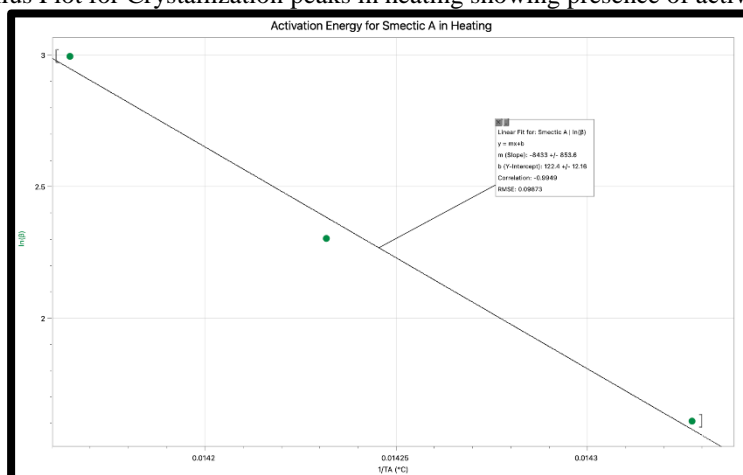


Figure 25. Arrhenius Plot for Smectic A in heating shows the presence of activation energy in it.

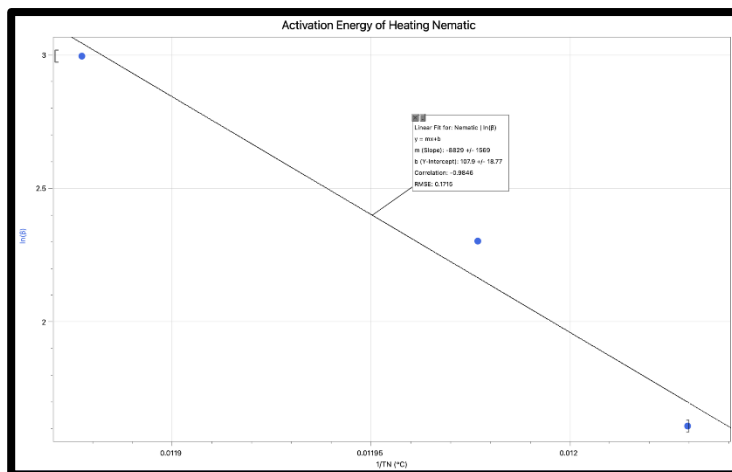


Figure 26. Arrhenius's Plot for Nematic in heating shows the presence of activation energy in it.

The increasing trend of seeing how the peaked temperatures of the liquid crystal change with an increasing ramp is further supported by the data found and Figures 23-26, which calculate the amount of activation energy used for each phase transition during heating exclusively. This relationship was derived using equation 5, which relates the rate of a reaction to its activation energy and coordinates its variables to represent a linear relationship found in equation 11. The values for these figures can be found in Table 3.

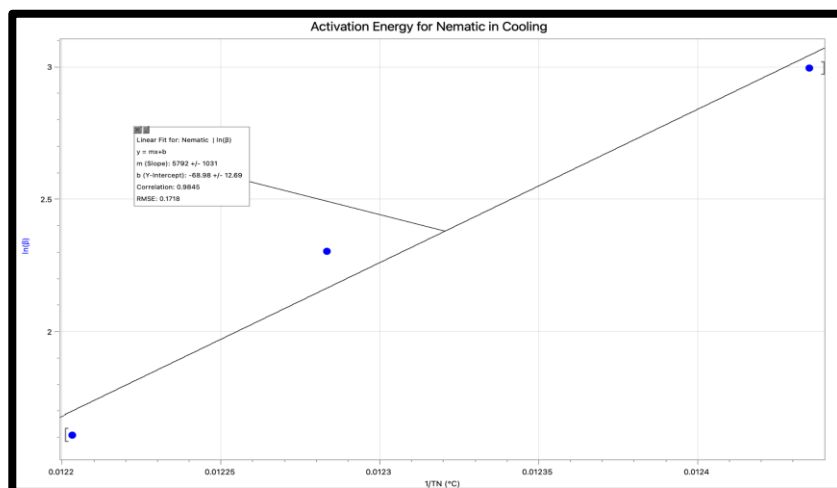


Figure 27. Arrhenius's Plot for Nematic in cooling shows the presence of activation energy in it. relationship of activation energy.

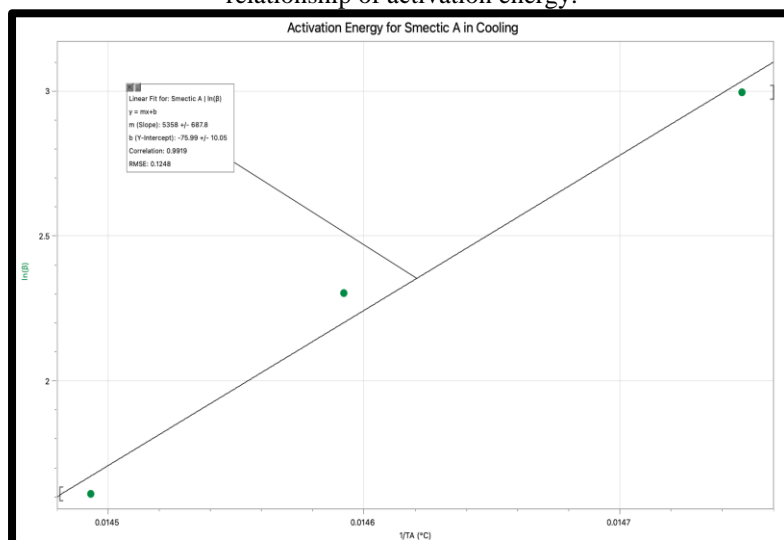


Figure 28. Arrhenius Plot for Smectic A in cooling showing the presence of activation energy in it.

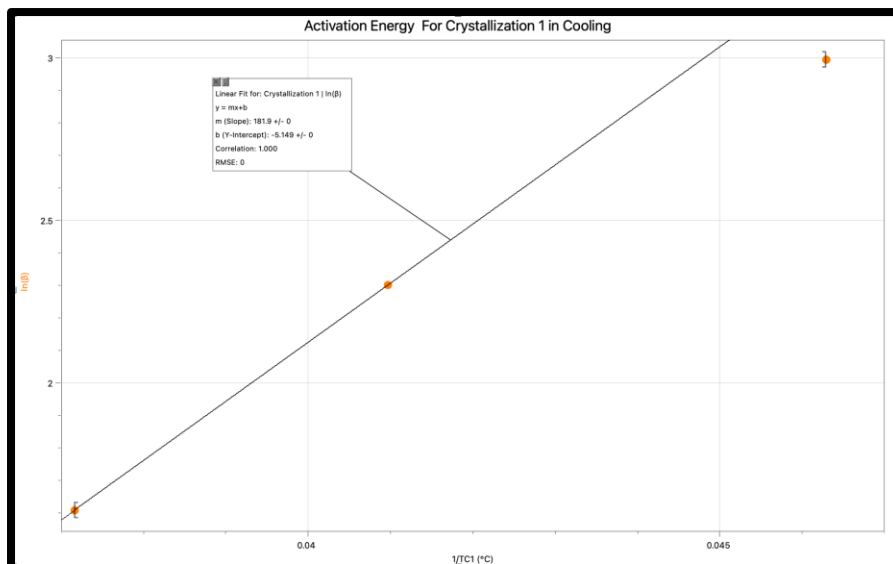


Figure 29. Arrhenius Plot for Crystallization 1 in cooling showing the presence of activation energy in it.

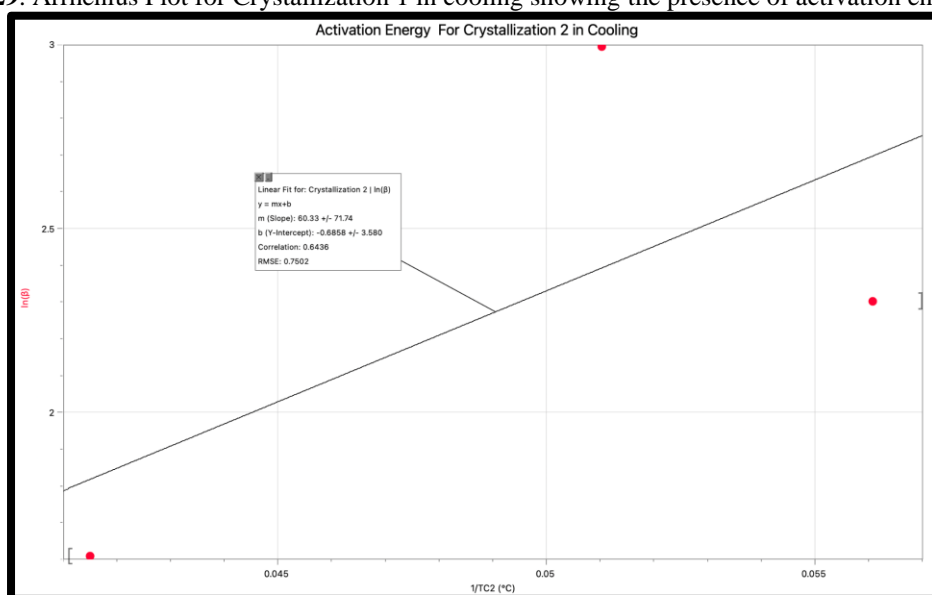


Figure 30. Arrhenius Plot for Crystallization 2 in cooling showing the presence of activation energy in it.

Figure 27-30 similarly represents the relationship of the ramp rates in the activation energy for each phase transition, except these graphical representations account for the cooling phases of 8OCB. The data for these graphs can be found in Table 3.

Table 3. Activation energy data related to Figures 23-30.

Transition	Slope=m	R/mol * K	Ea (kJ/mol)	Uncertainty of Ea (kJ/mol)	ln (Bo)	Uncertainty of ln (Bo)
Crystallization 0 (heat)	246.60	8.31	2.04	0.00	7.79	0.00
Crystallization 1 (heat)	429.10	8.31	3.56	0.05	11.12	1.12
Smectic A (Heat)	8433.00	8.31	70.07	0.85	122.40	12.60
Nematic (Heat)	8829.00	8.31	73.36	1.56	107.90	18.70
Nematic (Cool)	5792.00	8.31	48.13	1.03	-68.98	12.69
Smectic A (Cool)	5358.00	8.31	44.52	0.68	-75.99	10.05
Crystallization 1 (Cool)	150.50	8.31	1.25	0.01	-3.93	0.59

Crystallization 2(Cool)	60.33	8.31	0.50	0.07	-0.68	-3.58
-------------------------	-------	------	------	------	-------	-------

The calculated activation energy was determined using equation 5-11 where the inverse of the peak temperature was taken ($1/T$), and the natural log of the ramp rate was calculated ($\ln(B_0)$) and graph together, and the slope could be determined related to activation energy of equation 11 where the slope was multiplied by the gas constant ($R=8.31 \text{ J/mol} \cdot \text{K}$). The Y-intercept of the graph represents the value of $\ln(B_0)$ with its calculated uncertainties.

Table 4a-h. Changes in temperature, heat capacity, and wing jump for 8OCB heating and cooling at 5, 10, and 20°C/min. ΔT (°C) is the calculated change and temperature just before and after the transition. ΔC_p ((J/g)°C) is the difference in the height of the peak. WJ ((J/g)°C) is the calculated distance between the capacity before and after the peak transition. The preceding seven tables break up the data between the type of transitions and its corresponding ramp rates separated by heating and cooling.

Table 4a. Heating crystallization 1 data for 5, 10, and 20°C/min

Crystallization 0 (heat)			
Heating Rate (°C/min)	ΔT (°C)	ΔC_p ((J/g)°C)	WJ ((J/g)°C)
5			
10	3.56	0.23	0.16
20	19.60	1.34	0.71

Table 4b. Heating crystallization 2 data for 5, 10, and 20°C/min

Crystallization 1 (heat)			
Heating Rate (°C/min)	ΔT (°C)	ΔC_p ((J/g)°C)	WJ ((J/g)°C)
5	11.47	42.19	0.38
10	16.30	21.07	0.19
20	16.26	13.43	-0.074

Table 4c. Heating smectic A data for 5, 10, and 20°C/min

Smectic A			
Heating Rate (°C/min)	ΔT (°C)	ΔC_p ((J/g)°C)	WJ ((J/g)°C)
5	6.26	0.17	0.09
10	5.95	0.12	0.08
20	2.97	0.25	0.21

Table 4d. Heating nematic data for 5, 10, and 20°C/min

Nematic			
Heating Rate (°C/min)	ΔT (°C)	ΔC_p ((J/g)°C)	WJ ((J/g)°C)
5	11.73	2.58	-0.28
10	14.79	1.57	-0.17
20	19.62	0.95	-0.16

Table 4e. Cooling nematic data for 5, 10, and 20°C/min

Nematic			
Cooling Rate (°C/min)	ΔT (°C)	ΔC_p ((J/g)°C)	WJ ((J/g)°C)
5	-12.14	1.88	0.13
10	-14.36	1.56	0.11
20	-16.81	0.87	-0.14

Table 4f. Cooling smectic data for 5, 10, and 20°C/min

Smectic A			
Cooling Rate (°C/min)	ΔT (°C)	ΔC_p ((J/g)°C)	WJ ((J/g)°C)
5	-12.34	-0.64	-0.19
10	-12.34	-0.67	-0.19
20	-12.42	-0.14	-0.28

Table 4g. Cooling crystallization 1 data for 5, 10, and 20°C/min

Crystallization 1			
Cooling Rate (°C/min)	ΔT (°C)	ΔC_p ((J/g)°C)	WJ ((J/g)°C)
5	-3.25	14.54	-20.36
10	-13.40	28.54	0.24
20	-11.16	12.12	11.82

Table 4h. Cooling crystallization 2 data for 5, 10, and 20°C/min

Crystallization 2			
Cooling Rate (°C/min)	ΔT (°C)	ΔC_p ((J/g)°C)	WJ ((J/g)°C)
5	-1.76	0.35	-0.34
10	-6.75	-0.16	-0.62
20	-16.36	-0.64	-12.15

As the tables above in coordination with **Figures 23-30** corroborate the information in **Tables 1-2** that the phase transitions do, in fact, move when the ramp rates are increasingly introduced. During heating and cooling all transitions remain to have a lower activation energy than the nematic phase transition, supporting the nematic's stability and ability to handle the increasing influx of energy. All the phase transitions have decreased variability in activation energy even when exposed to increasing ramp rates. This data further supports the hypothesis that 8OCB would be a strong candidate for integration into LCD manufacturing as its stability aids in avoiding degradation.

As seen in **Table 4**, there are missing and added phase transitions during the heating and cooling phases. Notably, in heating, there is the addition of a heating crystallization peak while in the cooling phase, there is a subsequent absence of a crystallization peak. This is due to a phenomenon that when liquid crystal molecules are repeatedly reheated, they actually retain some of the energy from the previous cycle of heating and cooling. Due to this

increase in kinetic energy, the molecule showcases an additional phase transition during the reheating of the ramp rates 10 and 20. There's also the appearance of missing transitions during cooling, which is greatly highlighted as the distinct cooling crystallization phase transitions become less defined showcased in **Table 4** as the ΔC_p ((J/g) $^{\circ}C$) and WJ ((J/g) $^{\circ}C$) increase over more significant temperature differences. This can also be graphically seen in Figures 3-4.

Table 5. Change in enthalpy of each peak transition for heating of 8OCB at 5, 10, and 20 $^{\circ}C/min$.

Heating Rate ($^{\circ}C/min$)	ΔH (J/g) Crystallization	ΔH (J/g) Smectic A	ΔH (J/g) Nematic
5	100.85	0.17	3.78
10	87.85	0.17	3.54
20	83.64	0.01	3.52

Table 6. Change in enthalpy of each peak transition for cooling of 8OCB at 5, 10, and 20 $^{\circ}C/min$.

Cooling Rate ($^{\circ}C/min$)	ΔH (J/g) Nematic	ΔH (J/g) Smectic A	ΔH (J/g) Crystallization
5	3.83	0.22	69.91
10	3.55	0.12	78.10
20	3.70	0.11	75.96

Tables 5-6 catalogs the enthalpy of each phase transition, which interestingly shows that the heating crystallization phase increases its enthalpy values as the rates decrease, whereas the cooling crystallization phase relatively increases as the ramp rates increase. This data reveals a lot about why the phase transition peak temperatures move and why the number of phase transitions decreases relative to the increasing ramp rates. This enthalpy data also helps further explain the disappearance and appearance of crystallization peaks for the cooling crystallization phase change.

V. Discussion

Figures 31-32 are schematic representations that aid in understanding why the phase transitions move and the change in the loss or gain of phase transitions. From the first heating of the liquid crystal molecules, the crystal started at a genuine 100% crystallization state, where all the molecules exhibited complete order within their rows and columns. However, after being heated a second and third time, these liquid crystal molecules did not go back into their exact orientation, and there was an increase in peaks during the heating transition. This is best illustrated in Figure 26 in the crystalline state. This occurrence can also be seen in the LC 5OCB.[18]

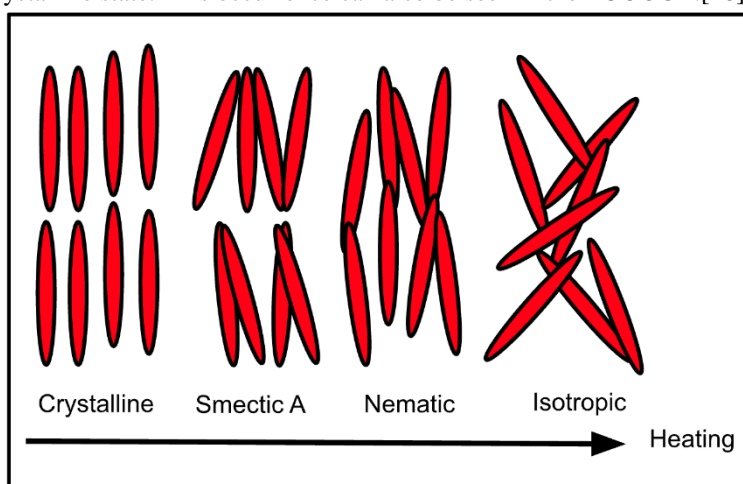


Figure 31. Schematic representing the predicted model of the molecular alignment of 8OCB for each phase transition during heating.

The additional heat retained within the molecules, even when cooled, starts the phase transition in an already slightly disorganized state. This helps further explain the decrease in activation energy during the heating transitions and the increase in activation energy during the cooling transitions seen in **Table 3**. Due to the system not being 100% crystallized upon the second reheating, liquid crystal molecules do not require as much heat to complete the phase transition and are also exhibiting further transition because of the additional heat within the system. This also applies to cooling as the activation-energy increases due to there being an increasingly higher amount of heat within the phase transitions that need to be released to cool down.

Table 4 reports the values of WJ, which can be seen at increasing and decreasing fluctuation between the phase transitions at different ramp rates, supporting the observation found in Figures 6-8 and 10-12, a pattern also seen amongst the mixture of LC 5CB+7CB and in the OCB family with 5OCB. [19-20] There are differences in the heat capacity before and after the phase transition as the molecules are not resorting to the same heat capacity post-phase transition by retaining some residual energy that relates to how the transition temperatures increase through increasing ramp rates. This lack in specificity in transitions then contributes to the loss of distinct peak transitions in the crystallization cooling phase of ramp rates 10 and 20 in **Table 2**, and the addition of heating crystallization peaks.

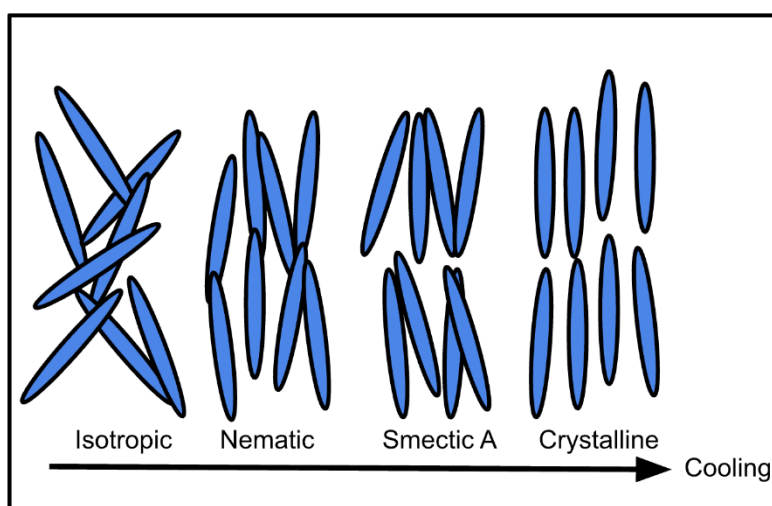


Figure 32. Schematic representing the predicted model of the molecular alignment of 8OCB for each phase transition during cooling.

VI. Conclusion

The paper explored the effects of ramp rates on 8OCB during continuous heating and cooling. 8OCB was heated from $-40\text{ }^{\circ}\text{C}$ to $100\text{ }^{\circ}\text{C}$ and then cooled back from $100\text{ }^{\circ}\text{C}$ to $-40\text{ }^{\circ}\text{C}$ with three different ramp rates of $5\text{ }^{\circ}\text{C}/\text{min}$, $10\text{ }^{\circ}\text{C}/\text{min}$, and $20\text{ }^{\circ}\text{C}/\text{min}$. From heating and cooling the molecules multiple times there were effects seen on various phase transitions [21]. The most affected were in heating/cooling crystallization, as seen in the temperature dynamics of the move phase transitions. The transitions during heating move towards higher temperatures when the ramp rate increases, while phase transitions during cooling move towards lower temperatures as the ramp rates increase. Most notably, the activation energies were affected due to this phenomenon. The smallest activation energies were amongst the crystallization phase changes, while the highest activation energies were found amongst the nematic phase transitions. This could also be seen in the enthalpy values found in Tables 5- 6, where the enthalpy was seen to decrease with each heating and increase with each cooling due to the retention of energy within the molecules. Most relevant to LCDs are the notably higher activation energy values for the nematic phase transition and why nematic phases are used in these types of displays due to their stability in handling rapid rates of heating and cooling. In the case of 8OCB, these findings support its candidacy for LCD integration as additional stability from oxygenated LCs would aid in preventing the degradation of the LCD.

Acknowledgments

The authors would like to acknowledge Professor John C. MacDonald from the Chemistry and Biochemistry department and Life Sciences and Bioengineering Center, WPI, Worcester, MA for providing Differential Scanning Calorimetry (DSC) model NETZSCH 214 instruments. The authors also like to acknowledge NETZSCH company for DSC 214 pans and lids. The student author would like to acknowledge Dr.

Dipti Sharma for supervising this research internship with Liquid Crystal, and Emmanuel College for running internship programs.

References

- [1]. Tin Win, D. (n.d.). States of Matter Part I. The Three Common States: Solid, Liquid, and Gas (p. 5). Assumption University Bangkok, Thailand.
- [2]. Schadt, M. (1997). Liquid crystal materials and liquid crystal displays. *Annual Review of Materials Science*, 27(1), 305–379. <https://doi.org/10.1146/annurev.matsci.27.1.305>
- [3]. Chen, H.-W., Lee, J.-H., Lin, B.-Y., Chen, S., & Wu, S.-T. (2017). Liquid crystal display and organic light-emitting diode display: Present status and future perspectives. *Light: Science & Applications*, 7(3), 17168–17168. <https://doi.org/10.1038/lsa.2017.168>
- [4]. Kobayashi, S., Miyama, T., Akiyama, H., Ikemura, A., & Kitamura, M. (2022). Development of liquid crystal displays and related improvements to their performances. *Proceedings of the Japan Academy. Series B, Physical and Biological Sciences*, 98(9), 493. <https://doi.org/10.2183/pjab.98.025>
- [5]. Gill, P., Moghadam, T. T., & Ranjbar, B. (2010). Differential scanning calorimetry techniques: Applications in biology and nanoscience. *Journal of Biomolecular Techniques: JBT*, 21(4), 167. <https://pubmed.ncbi.nlm.nih.gov/articles/PMC2977967/>
- [6]. S. Kumar, S.-W. Kang. (2005). Liquid crystals, encyclopedia of condensed matter. Physics. Elsevier, 111-120. 9780123694010
- [7]. Mitov, M. (2014). Liquid-crystal science from 1888 to 1922: Building a revolution. *Chemphyschem: A European Journal of Chemical Physics and Physical Chemistry*, 15(7), 1245–1250. <https://doi.org/10.1002/cphc.201301064>
- [8]. Sharma, D., & Farah, K. (2016). A review of nematic liquid crystals. *Trends in Physical Chemistry*, 16, 47–52.
- [9]. Sharma, D. M. (2010). Non-isothermal kinetics of melting and nematic to isotropic phase transitions of 5CB liquid crystal. *Journal of Thermal Analysis and Calorimetry*, 102(2), 627–632. <https://doi.org/10.1007/s10973-010-0837-2>
- [10]. Ghosh, S., & Roy, A. (2021). Crystal polymorphism of 8OCB liquid crystal consisting of strongly polar rod-like molecules. *RSC Advances*, 11(9), 4958. <https://doi.org/10.1039/d0ra08543j>
- [11]. Selevou, A., Papamokos, G., Steinhart, M., & Floudas, G. (2017). 8ocb and 8cb liquid crystals confined in nanoporous alumina: Effect of confinement on the structure and dynamics. *The Journal of Physical Chemistry B*, 121(30), 7382–7394. <https://doi.org/10.1021/acs.jpcc.7b05042>
- [12]. LeBrun, W., Sharma (PhD), D., & Supervisor, Emmanuel College, Boston, MA 02115 USA. (2024). Characterizing mesophase transitions of 8cb liquid crystal using dsc and logger pro. *Engineering and Technology Journal*, 09(07). <https://doi.org/10.47191/etj/v9i07.18>
- [13]. Sharma, D., MacDonald, J. M., & Iannacchione, G. S. (2006). Thermodynamics of activated phase transitions of 8CB: DSC and MC calorimetry. *Journal of Physical Chemistry B*, 110(33), 16679–16684. <https://doi.org/10.1021/jp062862d>
- [14]. Logger Pro™ 3. (n.d.). Vernier. Retrieved November 20, 2024, from <https://www.vernier.com/product/logger-pro-3/>
- [15]. Liquid crystal displays. (n.d.). Retrieved November 20, 2024, from <https://web.media.mit.edu/~stefan/liquid-crystals/node3.html>
- [16]. What is a liquid crystal display (Lcd)? Advantages & disadvantages | lenovo ca. (n.d.). Retrieved November 20, 2024, from <https://www.lenovo.com/ca/en/glossary/what-is-lcd/>
- [17]. Petrarca, G., Sharma (PhD), D., & Supervisor, Emmanuel College, Boston, MA 02115 USA. (2024). Isothermal and non-isothermal study of 8ocb liquid crystal using dsc and logger pro. *Engineering and Technology Journal*, 09(07). <https://doi.org/10.47191/etj/v9i07.19>
- [18]. Byrne, L. E., & Sharma, D. D. (2023). Effect of Heating and Cooling on 6CB Liquid Crystal Using DSC Technique. *Engineering And Technology Journal*, 8(9), 2740–2756. <https://doi.org/10.47191/etj/v8i9.04>
- [19]. Doran, M., & Sharma, D. (2022). Melting and Nematic Phase Transitions of a Next Generation “Binary Liquid Crystal System (BLCS)” 5CB+7CB using Logger Pro. *International Journal of Research in Engineering and Science*, 10(12), 462–483.
- [20]. Mello, J. (2022). Details of Nematic Phase Transition and Nematic Range of 5OCB Liquid Crystal using Logger Pro. *International Journal of Research in Engineering and Science*, 10(9), 197–217. <https://www.ijres.org/papers/Volume-10/Issue-9/1009197217.pdf>
- [21]. Mello, J., & Sharma, D. (2022). Effect of Reheating and Ramp Rates on Phase Transitions of 5OCB Liquid Crystal using Logger Pro. *International Journal of Research in Engineering and Science (IJRES)*, 10(9), 218–236.